AGU PUBLICATIONS

Geophysical Research Letters

RESEARCH LETTER
10.1002/2015GL065319

Special Section:
First Results from the MAVEN Mission to Mars

New observations of molecular nitrogen in the Martian upper atmosphere by IUVS on MAVEN

M. H. Stevens[1], J. S. Evans[2], N. M. Schneider[3], A. I. F. Stewart[3], J. Deighan[3], S. K. Jain[3], M. Crismani[3], A. Stiepen[3], M. S. Chaffin[3], W. E. McClintock[3], G. M. Holsclaw[3], F. Lefèvre[4], D. Y. Lo[5], J. T. Clarke[6], F. Montmessin[4], S. W. Bougher[7], and B. M. Jakosky[3]

[1]Space Science Division, Naval Research Laboratory, Washington, District of Columbia, USA, [2]Computational Physics, Inc., Springfield, Virginia, USA, [3]Laboratory for Atmospheric and Space Physics, University of Colorado at Boulder, Boulder, Colorado, USA, [4]LATMOS, CNRS/UPMC/UVSQ, Paris, France, [5]Lunar and Planetary Laboratory, University of Arizona, Tucson, Arizona, USA, [6]Center for Space Physics, Boston University, Boston, Massachusetts, USA, [7]Department of Atmospheric, Oceanic and Space Sciences, University of Michigan, Ann Arbor, Michigan, USA

Key Points:
- N_2 detected in the upper atmosphere of Mars by IUVS on MAVEN
- Tentative identification of N_2 Vegard-Kaplan band emission confirmed
- N_2 Lyman-Birge-Hopfield bands identified on Mars for the first time

Correspondence to:
M. H. Stevens,
michael.stevens@nrl.navy.mil

Citation:
Stevens, M. H., et al. (2015), New observations of molecular nitrogen in the Martian upper atmosphere by IUVS on MAVEN, *Geophys. Res. Lett.*, *42*, doi:10.1002/2015GL065319.

Received 10 JUL 2015
Accepted 21 SEP 2015

Abstract We identify molecular nitrogen (N_2) emissions in the Martian upper atmosphere using the Imaging Ultraviolet Spectrograph (IUVS) on NASA's Mars Atmosphere and Volatile EvolutioN (MAVEN) mission. We report the first observations of the N_2 Lyman-Birge-Hopfield (LBH) bands at Mars and confirm the tentative identification of the N_2 Vegard-Kaplan (VK) bands. We retrieve N_2 density profiles from the VK limb emissions and compare calculated limb radiances between 90 and 210 km against both observations and predictions from a Mars general circulation model (GCM). Contrary to earlier analyses using other satellite data, we find that N_2 abundances exceed GCM results by about a factor of 2 at 130 km but are in agreement at 150 km. The analysis and interpretation are enabled by a linear regression method used to extract components of UV spectra from IUVS limb observations.

1. Introduction

The relatively low abundance of molecular nitrogen (N_2) in the present Martian atmosphere has been a topic of great interest [e.g., *Dalgarno and McElroy*, 1970; *Brinkmann*, 1971; *Fox*, 1993]. Although it seems evident that concentrations of N_2 in the past were much higher than they are now [*McElroy et al.*, 1976], new observations of N_2 on Mars would improve calculations of its escape rate and its evolution from primordial concentrations [*Fox and Dalgarno*, 1980; *Fox*, 1993]. These observations would be particularly valuable above about 120 km, where the upper atmosphere diffusively separates. In this region of the atmosphere measurements from mass spectrometers on the Viking landers indicated that N_2/CO_2 increases from about 3 to 10% between 130 and 160 km [*Nier et al.*, 1976; *Nier and McElroy*, 1977].

Even though the ultraviolet spectrometer on Mariner 6 found no evidence of N_2 in the Martian upper atmospheric dayglow nearly 50 years ago [*Barth et al.*, 1969], interest in its detection by this means has nonetheless persisted. *Fox and Dalgarno* [1979] predicted overhead intensities of a variety of N_2 bands and suggested that the photoelectron excited Vegard-Kaplan (VK) bands in the mid-UV (MUV) may be detectable. In practice, however, the measurement is challenging because the N_2 dayglow emission is weak relative to the bright and spectrally complex emissions arising primarily from processes on CO_2 that are present throughout the MUV [e.g., *Jain et al.*, 2015].

Leblanc et al. [2006] reported a tentative identification of VK emission using limb observations from the Spectroscopy for the Investigation of the Characteristics of the Atmosphere of Mars (SPICAM) instrument on the Mars Express mission. *Leblanc et al.* [2007] later determined that the SPICAM VK emission was about 3 times weaker than predicted by *Fox and Dalgarno* [1979], suggesting that *Fox and Dalgarno* had overestimated these emissions and that new calculations using more recent parameters may resolve the discrepancy. *Fox and Hac* [2013] updated the calculations using the latest molecular constants, cross sections, and solar irradiance models and determined that revised predictions of limb intensities were indeed consistent with SPICAM observations. However, using a separate model calculation, *Jain and Bhardwaj* [2011] concluded that N_2 abundances must be about a factor of 3 smaller in order to reconcile the SPICAM observations with their results.

Table 1. IUVS Limb Observations for This Work

Date	18 October 2014
UT	16:44
MAVEN orbit	109
Solar zenith angle	44°
$F_{10.7}$	65
Local solar time	14.3
Latitude	12°N
Longitude	131°E
MAVEN latitude	15°N
MAVEN longitude	147°E
MAVEN altitude	320 km

Here we present new MUV observations of N_2 VK limb emission from the upper atmosphere of Mars using the Imaging Ultraviolet Spectrograph (IUVS) aboard NASA's Mars Atmosphere and Volatile EvolutioN (MAVEN) Mission. The VK radiances are extracted with a multiple linear regression (MLR) approach using templates for spectral components discussed herein. We compare the extracted limb emission to model results and present the first observations of N_2 Lyman-Birge-Hopfield (LBH) bands in the far-UV (FUV). First, we describe the IUVS limb observations, we follow that with a description of the spectral analysis and then compare model limb radiances against VK and LBH observations.

2. The Observations

The MAVEN satellite was launched on 18 November 2013 and arrived at Mars on 22 September 2014. It was inserted into an elliptical orbit, which is nominally about 175 km by 6200 km above the planet's surface [*Jakosky et al.*, 2015]. IUVS images the Martian atmosphere onto a 0.06° × 11° entrance slit using two channels: a FUV channel (110–190 km) and a MUV channel (180–340 nm). At periapsis IUVS scans the limb of the Martian upper atmosphere between about 225 and 90 km at a vertical resolution of ~5 km with the slit nearly parallel to the orbital plane. Additional details on the IUVS instrument may be found in *McClintock et al.* [2014].

MAVEN orbits Mars about 5 times a day, and the IUVS is mounted on an Articulated Payload Platform that orients the IUVS field of view toward the limb during each periapsis pass. IUVS obtains 12 limb scans per orbit, and we focus herein on one scan from 18 October 2014, obtained a day before the passage of comet Siding Spring [*Schneider et al.*, 2015] during MAVEN Orbit 109. The spectra are from Level 1C IUVS data which are averaged in regularly spaced 5 km altitude bins centered between 92.5 and 267.5 km. Relevant attributes of the observations used in this work are summarized in Table 1. Since the Martian dayglow is driven primarily by solar processes [e.g., *Fox and Dalgarno*, 1979], it is important to monitor the solar activity during the observations when comparing against model results. During the observations presented here, the Sun was moderately active with an $F_{10.7}$ radio flux of 171 solar flux units (1 SFU = 10^{-22} W m^{-2} Hz^{-1}) at one astronomical unit (AU). For these observations, Mars was 1.62 AU from the Sun so that the $F_{10.7}$ flux at Mars was 65 SFU.

3. Spectral Analysis

Both the MUV and FUV IUVS dayglow limb spectra are a blend of emissions arising primarily from solar processes on CO_2 and other minor species. We model the shape of each component and convolve them with the line spread function of the instrument. These template spectra are then simultaneously fit to the IUVS periapsis limb data (Version v03_r01) using MLR to isolate and extract the N_2 contribution. *Stevens et al.* [2011] used this approach successfully in the analysis of the Titan UV dayglow observed by the Cassini Ultraviolet Imaging Spectrograph (UVIS). We adapt the approach to Mars herein and discuss its application to the MUV VK bands next followed by the FUV LBH bands.

3.1. The MUV VK Bands

The MUV dayglow spectrum at Mars is dominated by the CO Cameron bands ($a^3\Pi - X^1\Sigma^+$; see *Jain et al.* [2015]). Although they are most prominent between 180 and 250 nm, there is Cameron band emission present longward of 250 nm where several photoelectron excited N_2 VK bands ($A\ ^3\Sigma^+ - X^1\Sigma^+$) are present. We select the wavelength region between 258.0 and 287.5 nm to retrieve the VK spectrum since two VK bands ((0,5) and (0,6)) have already been tentatively identified in this region [*Leblanc et al.*, 2006]. Even at

these longer wavelengths, the Cameron band emission can be brighter than the VK emission, so it is crucial to accurately simulate the Cameron band shape in order to remove its contribution to the signal.

The Cameron bands were modeled by *Conway* [1981] using the Mariner 9 dayglow data, and we adapt that approach here. *Conway* found that the rotational distribution of the bands observed by the ultraviolet spectrometer on board Mariner 9 could be approximated by a Boltzmann distribution at two different temperatures: one at 1600 K and one at 10,000 K. We find that the IUVS data fit better at lower temperatures than inferred from Mariner 9 data and herein use temperatures of 800 K ($J < 20$) and 6000 K ($J \geq 20$) for our analysis. Upper state vibrational populations are from *Conway* [1981] and branching ratios are from *James* [1971] for $v' = 0$ and $v' = 1$ and from *Conway* for $v' > 1$. Rotational and vibrational constants used in the synthesis of all the vibrational bands are from *Huber and Herzberg* [1979]. We model transitions from eight upper vibrational states and 15 lower vibrational states, as well as 180 rotational levels for each band.

The VK bands are modeled using the vibrational and rotational constants tabulated by *Huber and Herzberg* [1979] with line intensity factors from *Schlapp* [1937]. Upper state vibrational populations are from *Strickland et al.* [1999], which include the effects of cascade and quenching [*Gronoff et al.*, 2012]. Branching ratios between $v' = 0$–6 are from *Piper* [1993], and between $v' = 7$–11 from *Shemansky* [1969]. We include 11 upper vibrational states and 17 lower vibrational states as well as 40 rotational transitions for each vibrational band [*Stevens et al.*, 2011]. The bands are modeled throughout this work with a Boltzmann distribution and a characteristic temperature of 200 K.

As described above, the VK analysis is limited to the narrow spectral region between 258.0 and 287.5 nm, which minimizes the uncertainties introduced by the Cameron band two-temperature fit. Other important contributions modeled in this MUV spectral region include the CO_2^+ ultraviolet doublet (UVD) [*Evans et al.*, 2015], the CO_2^+ Fox-Duffendack-Barker (FDB) bands [*Farley and Cattolica*, 1996], and the O 297.2 nm line, which are all at longer wavelengths than the above spectral region [*Jain et al.*, 2015] but nonetheless contribute to the emission near 287 nm.

There are several additional components that contribute weakly. The CO^+ first negative bands are included and modeled following the approach of *Conway* [1981]. Any contribution due to solar scattered light from aerosols or dust is removed by including an observed spectrum of solar scattered light in the MLR. This spectrum is from a nadir-viewing IUVS dayglow observation of the Martian disk. Above 90 km tangent altitude, this contribution is weak. Occasionally, metal emissions (Mg^+, Mg, Fe^+, and Fe) can appear in the MUV spectrum, and these are also included in the MLR using the approach of *Schneider et al.* [2015]. As discussed by *Schneider et al.*, the metals dramatically appear following the passage of comet Siding Spring at Mars in late October 2014, but the data considered here are taken before closest approach of the comet so the metal emissions although included in the MLR are weak. Finally, we include a baseline offset in the MLR that accounts for small broadband variations such as uncertainties in the subtraction of the detector dark current.

We smooth each of the 11 contributions described above with the IUVS line spread function in order to include them as independent vectors to the MLR. The line spread function is determined from an extended nadir-viewing dayglow observation of the H Lyman-α line at 121.6 nm by IUVS early in the mission. The shape of the feature is modeled with two Voigt functions, and the spectral widths of these are modified until the most prominent features in the MUV dayglow spectrum are adequately fit (175–300 nm). The full width at half maximum (FWHM) that best fits the data varies from 1.1 nm near 175 nm to 1.0 nm near 300 nm and is generally consistent with prelaunch estimates [*McClintock et al.*, 2014].

Figure 1a shows an IUVS limb spectrum along with a composite fit from the MLR. The spectrum is from a tangent altitude of 127.5 km, which is near the airglow peak. The contribution from the Cameron bands is evident at the short wavelength end of the spectrum and that contribution is split out in Figure 1b. The combined contributions from CO_2^+ UVD, CO_2^+ FDB, and O 297.2 nm are evident at the long wavelength end, and those are split out in Figure 1c. Also evident near 261 nm and 276.5 nm are the N_2 VK (0,5) and VK (0,6) bands, respectively. These are overplotted on the residual spectrum in Figure 1d. The total VK radiance within the plotted wavelength region and the estimated uncertainty from the MLR for this contribution are indicated. We also tentatively identify the weaker VK (2,7) and VK (1,7) bands, which have not been identified in Martian airglow spectra heretofore.

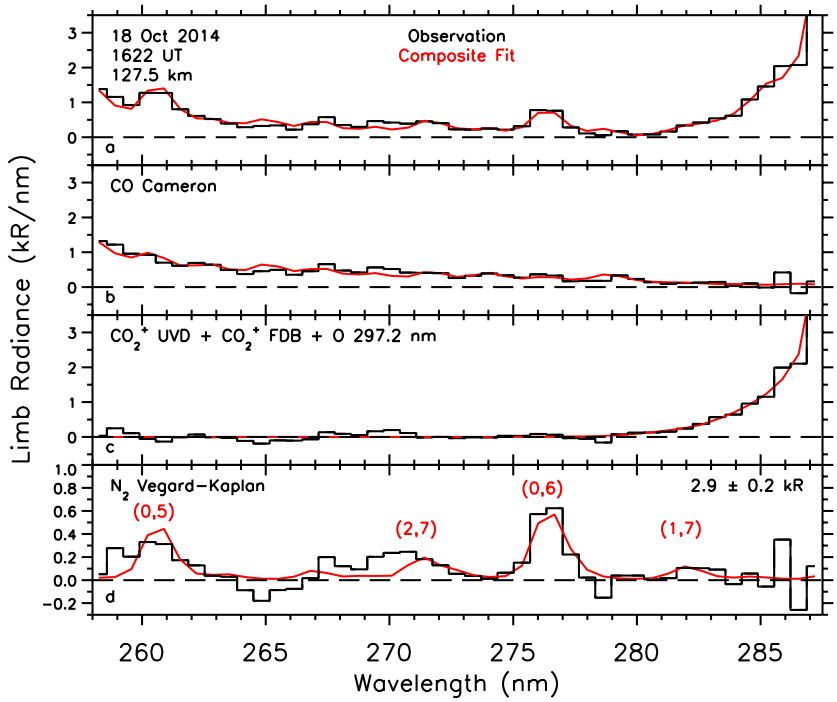

Figure 1. (a) An IUVS MUV limb spectrum (black histogram) near the airglow peak with the composite MLR fit overplotted (red). (b) The contribution from the CO Cameron bands, where the residual from the limb spectrum is shown with the MLR fit. (c). The total contribution from the CO_2^+ UVD, CO_2^+ FDB, and O 297.2 emission features. (d) The N_2 VK band residual, calculated by subtracting all other components to the MLR fit in Figure 1a. The modeled VK spectrum is overplotted in red, and the total radiance is indicated (note the change in scale).

3.2. The FUV LBH Bands

The photoelectron excited FUV N_2 LBH bands ($a^1\Pi_g - X^1\Sigma_g^+$) have never been identified in any Martian airglow spectra heretofore. This is primarily because they are weak relative to other blended FUV features. We use a similar approach to extract LBH radiances from the FUV limb spectra as we did in the MUV. Specifically, we identify all known components, model their spectral variation at high resolution, convolve the components with the instrument line spread function, and simultaneously fit them to the data in a targeted wavelength region using MLR (131.0–142.5 nm). The line spread function used is the IUVS FUV H Lyman-α observation of the Martian disk with a FWHM of 0.7 nm. As with the MUV, the wavelength scale and the dispersion relation are determined using multiple discrete features over a larger passband (114–168 nm), whereas the LBH radiance is determined in the narrow spectral region over which the emission is brightest.

The most prominent feature in the LBH spectral region selected above is the O 135.6 nm multiplet [*Jain et al.*, 2015]. We determine the wavelengths of the atomic multiplets from the National Institute of Standards and Technology database [http://www.nist.gov/pml/data/asd.cfm] and use the Einstein A values to describe their relative intensities. The bright O 130.4 nm multiplet is included in the MLR but is far enough away from the short wavelength edge of the targeted spectral region so that its contribution is negligible. Also included in the MLR are the C^+ multiplet at 133.6 nm as well as the carbon monoxide Fourth Positive (CO 4PG) bands [*Kurucz*, 1976; *Durance et al.*, 1980]. CO 4PG is primarily produced from two different processes: photodissociation and dissociative recombination. We use a different upper state vibrational population for each of these processes and fit them as independent components in the MLR. Also, since CO 4PG can be optically thick in the Martian upper atmosphere we additionally split these two components into optically thick bands that terminate on the ground state ($v'' = 0$) and optically thin bands ($v'' > 0$). For the LBH spectral region, only the optically thick CO 4PG bands are present and their contribution from both sources is small but is nonetheless included in the MLR. Similarly, the C multiplet at 132.9 nm identified in previous data sets [*Barth et al.*, 1971] is included in the MLR, but its contribution is very small. The vibrational and rotational structures of the LBH bands are modeled following the approach of *Conway* [1982] at a temperature of 295 K throughout the Martian atmosphere.

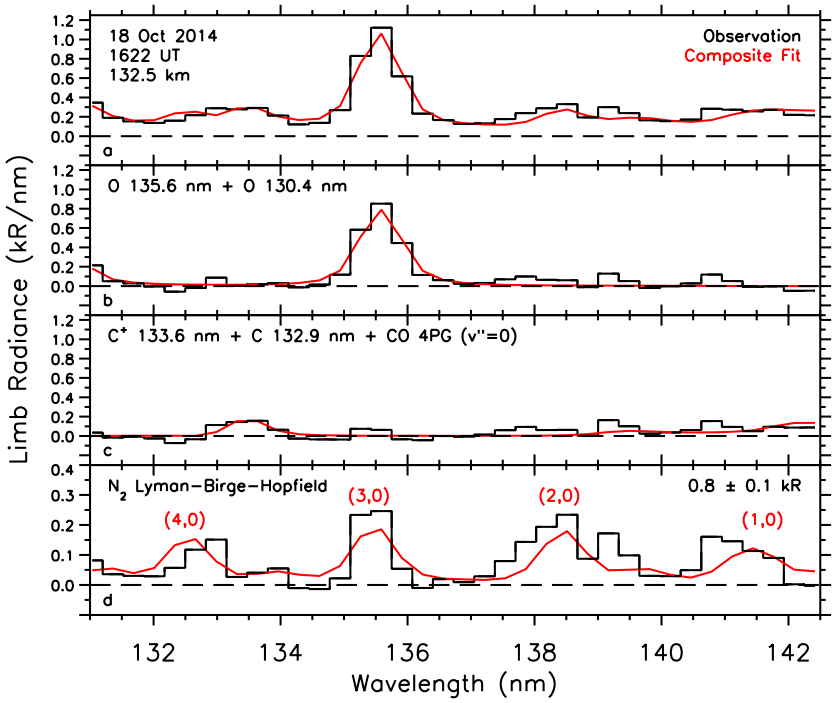

Figure 2. (a) An IUVS FUV limb spectrum (black histogram) near the airglow peak with the composite MLR fit overplotted (red) from the same scan as used in Figure 1. (b). The contribution from the O 135.6 nm multiplet, where the residual from the limb spectrum is shown with the MLR solution. (c) The contribution from C^+ 133.6 nm and the optically thick solution ($v'' = 0$) for CO 4PG. (d) The residual LBH spectrum and the modeled LBH spectrum, where the total LBH radiance is indicated (note the change in scale).

Figure 2a shows an IUVS FUV spectrum from the Martian dayglow at a tangent altitude of 132.5 km for the same scan as used in Figure 1. The O 135.6 nm multiplet is prominent near the middle of the spectrum, and this feature is split out from the data in Figure 2b. Figure 2c shows the other smaller contributions to this portion of the spectrum, including the C^+ 133.6 nm feature and the CO 4PG bands. Finally, Figure 2d shows the residual N_2 LBH spectrum as well as the MLR fit overplotted. The total LBH limb radiance for this spectral region is indicated as well as the estimated uncertainty from the MLR. Four prominent LBH features clearly rise above the noise and are coincident with the expected feature positions as indicated by the fit, and we identify them as the (4,0), (3,0), (2,0), and (1,0) bands [*Conway*, 1982; *Stevens et al.*, 2011].

4. Results

We extract the VK radiance from the MUV limb data as well as the LBH radiance from the FUV data in 5 km increments from 90 to 210 km. The resultant limb profile is shown in Figure 3, where the uncertainties are obtained from the MLR fits at each altitude. IUVS was calibrated against UV-bright stars and scaled by instrument geometric factors appropriate for extended source observations. The MUV systematic uncertainty estimated from these stellar calibrations is ±30%, and retrieved N_2 limb radiances and densities using the VK bands are linearly dependent on this uncertainty [*Evans et al.*, 2015]. The FUV systematic uncertainty is estimated to be ±25%.

The VK limb radiances are inverted to retrieve a N_2 density profile using an algorithm described by *Stevens et al.* [2015] for UVIS observations of Titan's upper atmosphere, which is dominated by N_2. The application of the N_2 density retrieval to the upper atmosphere of Mars and the forward model calculation using the N_2 bands described herein is discussed in *Evans et al.* [2015]. *Stevens et al.* showed that Titan N_2 density retrievals constrained only by photofragmented multiplets (N^+ 108.5 nm and N 149.3 nm) yield model limb radiances that also agree well with VK and LBH observations, indicating a consistent understanding between these three sets of emissions in a N_2-dominated atmosphere. This underscores the value of the VK bands for retrieving N_2 densities from the Martian UV dayglow.

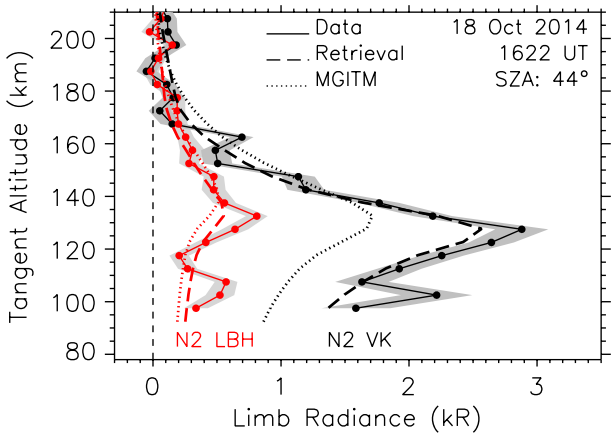

Figure 3. Observed integrated limb radiances for the N_2 VK bands (258.0–287.5 nm) and the N_2 LBH bands (131.0–142.5 nm). The solar zenith angle (SZA) is shown in the upper right. The shaded area indicates the 1-σ uncertainty of the retrieval. Overplotted (dashed lines) are calculated limb radiances for the VK and LBH bands [*Stevens et al.*, 2015; *Evans et al.*, 2015]. The LBH model radiances are based only on the N_2 density retrieval from the VK bands. Also overplotted (dotted lines) are predictions from a Mars general circulation model, which are significantly less than observations near the airglow peak at 130 km.

The converged solution in Figure 3 agrees well with the VK observations at almost all altitudes shown. Using this N_2 retrieval we show the predicted limb radiance profile for the LBH emission. We emphasize that this forward model result is not constrained by the IUVS LBH observations and relies only on the N_2 density profile retrieved from VK observations. Nonetheless, the remarkable agreement is on average within 15% and provides additional evidence that the LBH bands are identified in the Martian upper atmosphere.

Also shown in Figure 3 are calculated limb radiance profiles using N_2 densities from the Mars Global Ionosphere-Thermosphere Model (M-GITM) [*Bougher et al.*, 2015; *Evans et al.*, 2015], for the conditions consistent with those indicated in Table 1. The figure shows that predicted VK limb radiances are significantly less than observations near the airglow peak at 130 km but more consistent with observations near 150 km. LBH radiances are less sensitive to N_2 density changes due to CO_2 opacity on the limb in the FUV [*Yoshino et al.*, 1996]. The retrieved N_2 abundance at 130 km (2.9×10^9 cm^{-3}) is a factor of 2.5 more than the M-GITM results at the same altitude and for the same scan. Analyses of a month of limb scan data from IUVS indicates that on average the retrieved N_2 densities are less than this but still exceed the M-GITM results by about a factor of 2 with a significant amount of variability about the mean (~50%). We find that the discrepancy with M-GITM results is altitude dependent so that near 150 km the retrieved N_2 abundance (2.3×10^8 cm^{-3}) is generally in agreement with M-GITM results. Retrieved N_2 densities that are a factor of 3 less than predictions [e.g., *Jain and Bhardwaj*, 2011] are not supported by these IUVS data. Comparison of N_2 mixing ratios with M-GITM results can be done through the retrieval of CO_2 densities from the CO_2^+ ultraviolet doublet near 289 nm, and this is discussed further in *Evans et al.* [2015].

5. Conclusions

We have shown that the spectral content of the Martian UV dayglow can be disambiguated if each contribution is separately identified and simulated. We synthesize all of the spectral components from both an atomic line database and models that include the rotational and vibrational structure of the known molecular emissions. Weaker emissions such as those from N_2 are extracted by systematically removing the blended contributions as shown in Figures 1 and 2. The MLR approach implicitly requires an accurate description of the wavelength scales, the IUVS dispersion relation, and the line spread function of the instrument, and all of these are constrained by IUVS observations of the Martian dayglow in late 2014. Through analyses of VK limb radiance profiles, we find that retrieved N_2 number densities generally exceed general circulation model predictions by about a factor of 2 at 130 km but are in agreement near 150 km.

We have focused this study on a single 2 min scan from the first orbit of IUVS limb observations on 18 October 2014. From this scan, we identify four N_2 LBH bands (Figure 2d) which have not been identified at Mars before and tentatively identify two additional VK features also not identified at Mars before (Figure 1d). IUVS continues to observe the limb, and these observations will clarify the vertical, horizontal, and temporal variation of the N_2 abundance and mixing ratio in the Martian upper atmosphere [e.g., *Evans et al.*, 2015].

Acknowledgments

The MAVEN project is supported by NASA through the Mars Exploration Program. M.H.S. was supported by the NASA MAVEN Participating Scientist program. A. Stiepen is supported by the Belgian American Educational Foundation and Rotary District 1630. We thank F. Leblanc for many discussions from which this work benefited. The data are publicly archived at the Planetary Atmospheres node of the Planetary Data System (http://atmos.nmsu.edu/data_and_services/atmospheres_data/MAVEN/maven_iuvs.html).

The Editor thanks Phil Richards and an anonymous reviewer for their assistance in evaluating this paper.

References

Barth, C. A., W. G. Fastie, C. W. Hord, J. B. Pearce, K. K. Kelly, A. I. G. Stewart, E. Thomas, G. P. Anderson, and O. F. Raper (1969), Mariner 6: Ultraviolet spectrum of Mars upper atmosphere, *Science*, *165*, 1004–1005.

Barth, C. A., A. I. Stewart, C. W. Hord, and A. L. Lane (1971), Mariner 6 and 7 ultraviolet spectrometer experiment: Upper atmosphere data, *J. Geophys. Res.*, *76*, 2213–2227, doi:10.1029/JA076i010p02213.

Bougher, S. W., D. Pawlowski, J. M. Bell, S. Nelli, T. McDunn, J. R. Murphy, M. Chizek, and A. Ridley (2015), Mars global ionosphere thermosphere model (M-GITM): I. solar cycle, seasonal, and diurnal variations of the upper atmosphere, *J. Geophys. Res. Planets*, *120*, 311–342, doi:10.1002/2014JE004715.

Brinkmann, R. T. (1971), Mars: Has nitrogen escaped?, *Science*, *174*, 944–945.

Conway, R. R. (1981), Spectroscopy of the Cameron bands in the Mars airglow, *J. Geophys. Res.*, *86*, 4767–4775, doi:10.1029/JA086iA06p04767.

Conway, R. R. (1982), Self-absorption of the N_2 Lyman-Birge-Hopfield bands in the far ultraviolet dayglow, *J. Geophys. Res.*, *87*, 859–866, doi:10.1029/JA087iA02p00859.

Dalgarno, A., and M. B. McElroy (1970), Mars: Is nitrogen present?, *Science*, *170*, 167–168.

Durance, S. T., C. A. Barth, and A. I. F. Stewart (1980), Pioneer Venus observations of the Venus dayglow spectrum 1230–1430 Å, *Geophys. Res. Lett.*, *7*, 222–224, doi:10.1029/GL007i003p00222.

Evans, J. S., et al. (2015), Retrieval of CO_2 and N_2 in the Martian thermosphere using dayglow observations by IUVS on MAVEN, *Geophys. Res. Lett.*, *42*, doi:10.1002/2015GL065489.

Farley, D. R., and R. J. Cattolica (1996), Electron-beam fluorescence from the $A^2\Pi_u \rightarrow X^2\Pi_g$ and $B^2\Sigma_u^+ \rightarrow X^2\Pi_g$ transitions of CO_2^+, *J. Quant. Spectrosc. Radiat. Transfer*, *56*, 83–96.

Fox, J. L. (1993), The production and escape of nitrogen atoms on Mars, *J. Geophys. Res.*, *98*, 3297–3310, doi:10.1029/92JE02289.

Fox, J. L., and A. Dalgarno (1979), Ionization, luminosity, and heating of the upper atmosphere of Mars, *J. Geophys. Res.*, *84*, 7315–7333, doi:10.1029/JA084iA12p07315.

Fox, J. L., and A. Dalgarno (1980), The production of nitrogen atoms on Mars and their escape, *Planet. Space Sci.*, *28*, 41–46.

Fox, J. L., and N. E. F. Hac (2013), Intensities of the Martian N_2 electron-impact excited dayglow emissions, *Geophys. Res. Lett.*, *40*, 2529–2533, doi:10.1002/grl.50435.

Gronoff, G., C. Simon Wedlund, C. J. Mertens, M. Barthélemy, R. J. Lillis, and O. Witasse (2012), Computing uncertainties in ionosphere-airglow models. II—The Martian airglow, *J. Geophys. Res.*, *117*, A05309, doi:10.1029/2011JA017308.

Huber, K. P., and G. Herzberg (1979), *Constants of Diatomic Molecules*, Van Nostrand Reinhold Co., New York.

Jain, S. K., and A. Bhardwaj (2011), Model calculation of N_2 Vegard-Kaplan band emissions in Martian dayglow, *J. Geophys. Res.*, *116*, E07005, doi:10.1029/2010JE003778.

Jain, S. K., et al. (2015), Preliminary analysis of Martian dayglow observed by the Imaging Ultraviolet Spectrograph onboard MAVEN, *Geophys. Res. Lett.*, *42*, doi:10.1002/2015GL065419.

Jakosky, B. M., et al. (2015), The Mars Atmosphere and Volatile EvolutioN (MAVEN) mission, *Space Sci. Rev.*, doi:10.1007/s11214-015-0139-x.

James, T. C. (1971), Transition moments, Franck-Condon factors, and lifetimes of forbidden transitions—Calculation of the intensity of the Cameron system of CO, *J. Chem. Phys.*, *15*, 4118–4124.

Kurucz, R. L. (1976), *The Fourth Positive System of Carbon Monoxide*, *Smithson. Astrophys. Obs. Spec. Rep.*, vol. 374, SAO, Cambridge.

Leblanc, F., J. Y. Chaufray, J. Lilensten, O. Witasse, and J.-L. Bertaux (2006), Martian dayglow as seen by the SPICAM UV spectrograph on Mars Express, *J. Geophys. Res.*, *111*, E09S11, doi:10.1029/2005JE002664.

Leblanc, F., J. Y. Chaufray, and J. L. Bertaux (2007), On Martian nitrogen dayglow emission observed by SPICAM UV spectrograph/Mars Express, *Geophys. Res. Lett.*, *34*, L02206, doi:10.1029/2006GL028437.

McClintock, W. E., N. M. Schneider, G. M. Holsclaw, J. T. Clarke, A. C. Hoskins, I. Stewart, F. Montmessin, R. V. Yelle, and J. Deighan (2014), The Imaging Ultraviolet Spectrograph (IUVS) for the MAVEN mission, *Space Sci. Rev.*, doi:10.1007/s11214-014-0098-7.

McElroy, M. B., Y. L. Yung, and A. O. Nier (1976), Isotopic composition of nitrogen: Implications for the past history of Mars' atmosphere, *Science*, *194*, 70–72.

Nier, A. O., and M. B. McElroy (1977), Composition and structure of Mars' upper atmosphere: Results from the neutral mass spectrometers on Viking 1 and 2, *J. Geophys. Res.*, *82*, 4341–4349, doi:10.1029/JS082i028p04341.

Nier, A. O., et al. (1976), Composition and structure of the Martian atmosphere: Preliminary results from Viking 1, *Science*, *193*, 786–788.

Piper, L. G. (1993), Reevaluation of the transition-moment function and Einstein coefficients for the $N_2(A^3\Sigma_u^+ - X^1\Sigma_g^+)$ transition, *J. Chem. Phys.*, *99*, 3174–3181.

Schlapp, R. (1937), Fine structure in the $^3\Sigma$ ground state of the oxygen molecule, and the rotational intensity distribution in the atmospheric oxygen band, *Phys. Rev.*, *51*, 342–345.

Schneider, N. M., et al. (2015), MAVEN IUVS observations of the aftermath of the Comet Siding Spring meteor shower on Mars, *Geophys. Res. Lett.*, *42*, 4755–4761, doi:10.1002/2015GL062863.

Shemansky, D. E. (1969), N_2 Vegard-Kaplan system in absorption, *J. Chem. Phys.*, *51*, 689–700.

Stevens, M. H., et al. (2011), The production of Titan's ultraviolet nitrogen airglow, *J. Geophys. Res.*, *116*, A05304, doi:10.1029/2010JA016284.

Stevens, M. H., J. Scott Evans, J. Lumpe, J. H. Westlake, J. M. Ajello, E. Todd Bradley, and L. W. Esposito (2015), Molecular nitrogen and methane density retrievals from Cassini UVIS dayglow observations of Titan's upper atmosphere, *Icarus*, *247*, 301–312.

Strickland, D. J., J. Bishop, J. S. Evans, T. Majeed, P. M. Shen, R. J. Cox, R. Link, and R. E. Huffman (1999), Atmospheric Ultraviolet Radiance Integrated Code (AURIC): Theory, software architecture, inputs, and selected results, *J. Quant. Spectros. Radiat. Transfer*, *62*, 689–742.

Yoshino, K., J. R. Esmond, Y. Sun, W. H. Parkinson, K. Ito, and T. Matsui (1996), Absorption cross section measurements of carbon dioxide in the wavelength region 118.7–175.5 nm and the temperature dependence, *J. Quant. Spectrosc. Radiat. Transfer*, *55*, 53–60.